MULTIFREQUENCY EPR STUDY OF RADIATION-INDUCED DEFECTS IN CHLORAPATITE

Sergiy M. Nokhrin and Yuanming Pan[§]

Department of Geological Sciences, University of Saskatchewan, Saskatoon, Saskatchewan S7N 5E2, Canada

John A. Weil

Department of Chemistry, University of Saskatchewan, Saskatoon, Saskatchewan S7N 1C6, Canada

Mark J. Nilges

Illinois EPR Research Center, University of Illinois at Urbana-Champaign, Illinois 61801, U.S.A.

Abstract

Gamma-irradiated chlorapatite, synthesized from a $CaCl_2$ flux, has been investigated by powder and single-crystal electron paramagnetic resonance (EPR) spectroscopy at X- and W-band frequencies, including *in situ* high-T X-band EPR. The powder EPR spectra, particularly high-T X-band spectra and high-resolution W-band spectra, reveal a new hole-like center, H(III), in addition to two previously reported hole-like centers, H(I) and H(II). Center H(III) is characterized by an electron spin ½ and hyperfine interaction with one ^{35}Cl nucleus, suggesting a structural model consisting of a hole trapped by a substitutional oxygen ion adjacent to a Cl^- ion vacancy in the anion column. This discovery of center H(III) also lends support to the structural model already proposed by other authors for center H(II). Single-crystal X-band EPR spectra also disclose a new electronic center, E(I). The structure model for center E(I) includes an electron trapped at an isolated Cl^- ion vacancy in the anion column, corresponding to center $^FE(II)$ in fluorapatite and similar to the well-known F center in alkali halides.

Keywords: chlorapatite, electron-spin resonance spectra, radiation-induced defects.

Sommaire

Nous avons irradié la chlorapatite, synthétisée à partir d'un fondant $CaCl_2$, avec des rayons gamma, et nous en avons étudié les spectres de résonance des électrons paramagnétiques (EPR) prélevés sur poudre et sur monocristal aux fréquences des bandes X et W, y inclus la bande X à température élevée et *in situ*. Les spectres prélevés sur poudre, en particulier les spectres de la bande X à haute température et les spectres de haute résolution de la bande W, révèlent un nouveau centre semblable à un trou, H(III), en plus de deux centres semblables déjà connus, H(I) et H(II). Le centre H(III) possède un spin électronique ½ et une interaction hyperfine avec un nucléus ^{35}Cl, ce qui concorde avec un modèle structural impliquant un trou piégé par un atome d'oxygène substitutionnel voisin d'une lacune dans la colonne d'anions, site autrement occupé par l'ion Cl^-. Cette découverte du centre H(III) concorde aussi avec le modèle structural proposé antérieurement pour le centre H(II) par d'autres auteurs. Les spectres de la bande X prélevés sur monocristaux dévoilent aussi un nouveau centre électronique, E(I). Le modèle structural pour ce centre propose un électron piégé dans une lacune Cl^- isolée dans la colonne d'anions, correspondant au centre $^FE(II)$ de la fluorapatite et semblable au centre F bien connu dans les halogénures alcalins.

(Traduit par la Rédaction)

Mots-clés: chlorapatite, résonance des électrons paramagnétiques, défauts dus à l'irradiation.

§   *E-mail address*: yuanming.pan@usask.ca

INTRODUCTION

The apatite-group minerals having the general formula $Ca_{10}(PO_4)_6X_2$, where X represents F, Cl and OH, are ubiquitous in igneous, metamorphic and sedimentary rocks, and are major constituents in teeth, bones and vertebrate fossils (McConnell 1973, Elliott 1994, Pan & Fleet 2002). Fluorapatite has a $P6_3/m$ structure consisting of three types of cation polyhedra [Ca1O$_9$, Ca2O$_6$F and PO$_4$; Hughes & Rakovan (2002) and references therein]. Pure hydroxylapatite and chlor-apatite are monoclinic ($P2_1/b$) at room temperature, but undergo a phase transition to a hexagonal structure in the range ~200–350°C (Bauer & Klee 1993, Elliott 1994). Hughes & Rakovan (2002) emphasized that the Ca1O$_9$ polyhedron and the PO$_4$ tetrahedron remain essentially invariant in response to the incorporation of various X anions in the three end-members, whereas the Ca2O$_6$X polyhedron shows large shifts in the position of the X anions in the [00z] anion column. In particular, fluorine lies on the plane defined by three Ca2 atoms at z = 1/4 or 3/4, whereas OH$^-$ and Cl$^-$ are too large to be accommodated by the rigid Ca2 plane and hence are displaced above or below the plane. This ordering of OH$^-$ and Cl$^-$ in the anion column is responsible for the monoclinic symmetry of pure hydroxylapatite and chlorapatite (Hughes & Rakovan 2002). Most natural examples of chlorapatite and all known natural examples of hydroxylapatite, however, contain significant amounts of impurities and vacancies in the anion column that destroy this order; hence these are hexa-gonal. Bauer & Klee (1993) noted that even in pure synthetic chlorapatite, its phase-transition temperature varies with the sample's thermal history. They attributed this variation to differences in the amount of vacancies in the anion column. Therefore, nonstoichiometry in the anion column not only determines the symmetry of the apatite-group minerals, but also is known to have marked effects on their physical and chemical properties (*e.g.*, luminescence, exchange capacity, *etc.*), which are of considerable relevance to their applications in many areas of sciences and technology, from Earth sciences to agriculture, immobilization of heavy-metal ions and radioactive wastes, medical sciences and material sciences. Numerous previous studies have been made to characterize the anion column in the apatite-group minerals (Elliott 1994, Pan & Fleet 2002, and references therein).

In this contribution, we report on the results of a multifrequency (X- and W-band) EPR study of gamma-irradiated flux-grown chlorapatite, including *in-situ* X-band EPR experiments at high temperatures (up to 323°C). These EPR spectra, particularly the high-resolution W-band spectra and the high-T X-band spectra, allow identification of two new defect centers in chlorapatite. Spin-hamiltonian parameters from quantitative analysis of the X- and W-band EPR spectra allow us to provide structural models for the two new

defect centers and to re-evaluate the structural models of Knottnerus *et al.* (1972) and Roufosse *et al.* (1974) for the two known centers.

BACKGROUND INFORMATION

Electron paramagnetic resonance (EPR) spectros-copy has been proven to be particularly powerful in providing detailed structural information about dilute concentrations of paramagnetic defects in the anion column in fluorapatite (Segall *et al.* 1962, Piper *et al.* 1965, Warren 1972, Pan & Fleet 2002). For example, Piper *et al.* (1965) and Warren (1972) reported four electron-like centers [^{F}E(I), ^{F}E(II), ^{F}E(III) and ^{F}E(IV)] and four hole-like centers [^{F}H(I), ^{F}H(II), ^{F}H(III) and ^{F}H(IV)] in X-irradiated fluorapatite; the presuperscript denotes radiation-induced defect centers in fluorapatite (Fig. 1). The electron-like centers are associated with F$^-$ vacancies or substituting O^{2-} ions in the anion column: ^{F}E(I) is an electron trapped by one of two F$^-$ vacancies separated by a substitutional O^{2-} ion, ^{F}E(II) is an electron trapped by an isolated F$^-$ vacancy, ^{F}E(III) is an electron trapped by two F$^-$ vacancies adjacent to a substitutional O^{2-} ion, and ^{F}E(IV) an electron trapped by a F$^-$ vacancy adjacent to a substitutional O^{2-} ion. Piper *et al.* (1965) also reported a diamagnetic center (^{F}B) with two electrons trapped by two F$^-$ vacancies adjacent to a substitutional O^{2-} ion. Center ^{F}H(I) involves a hole trapped by a substitutional O^{2-} ion associated with a neighboring F$^-$ vacancy (Segall *et al.* 1962), whereas ^{F}H(II) consists of a hole trapped by an isolated substi-tutional O^{2-} ion. Piper *et al.* (1965) noted that ^{F}H(III) and ^{F}H(IV) form during the thermal conversion from ^{F}H(I) to ^{F}H(II). They interpreted ^{F}H(III) and ^{F}H(IV) to represent stable intermediate configurations during the progressive loss of the F$^-$ vacancy from the neighboring O^{2-} ion.
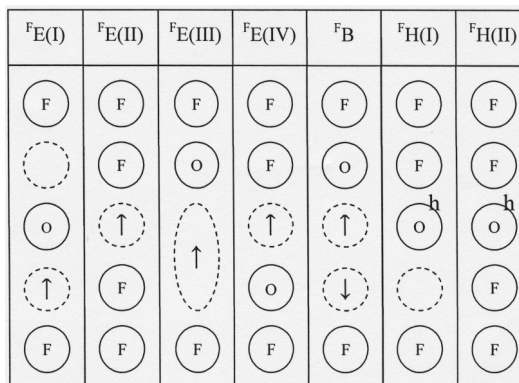

Fig. 1.   Structural models of color electron-like and hole-like centers in fluorapatite (after Segall *et al.* 1962, Piper *et al.* 1965, Warren 1972). The symbols "↑" and "↓" represent trapped electrons; "h" represents a trapped hole.

Similarly, defect centers in the anion columns of hydroxylapatite and chlorapatite have been investigated by EPR studies (Knottnerus *et al.* 1972, Roufosse *et al.* 1974, Mengeot *et al.* 1975, Pan & Fleet 2002, and references herein). For example, Mengeot *et al.* (1975) reported a spin-½ hole-like center exhibiting hyperfine interaction with a hydrogen nucleus (confirmed by deuteration) in X-irradiated hydroxylapatite. They attributed this center to an O^- ion arising from the removal of hydrogen from an OH^- ion, and suggested that the hyperfine interaction is with the hydrogen of an adjacent OH^- ion. Knottnerus *et al.* (1972) and Roufosse *et al.* (1974) both reported two oxygen-associated hole-like centers in X-irradiated flux-grown crystals of chlorapatite. It is noteworthy that the single-crystal EPR spectra in Roufosse *et al.* (1974) are similar to those of their respective centers in Knottnerus *et al.* (1972). However, these two groups of investigators reported different spin-hamiltonian parameters and disagreed in the proposed structural models.

EXPERIMENTAL PROCEDURES

Synthesis experiment

Chlorapatite, $Ca_{10}(PO_4)_6Cl_2$, was prepared as part of a program of syntheses for U-doped apatite-group minerals or analogues, following the flux method of Prener (1967). The starting materials were CaO (obtained from the decomposition of $CaCO_3$ at 900°C), P_2O_5 and $CaCl_2$ from the Sigma-Aldrich Chemical Company, and UO_2 from Alfa Aesar, were weighed and mixed thoroughly to form the composition of chlorapatite with approximately 10 ppm U. This mixture (11.75 g), together with flux materials (30 g $CaCl_2$), was then placed in a tightly covered 50 mL platinum crucible. The synthesis was carried out under atmospheric pressures in a Thermolyne muffle furnace equipped with a programmable controller. The mixture was first heated to 1280°C and held there for 24 hours to ensure complete melting and homogenization, and was then cooled down to 1060°C at a rate of 2°C/h and quenched in water. The resulting products contained several large crystals (up to 1 cm in length and ≥2 mm in diameter) and numerous smaller grains of chlorapatite, in a quenched melt of $CaCl_2$. The $CaCl_2$ was removed readily by washing in hot water. Chlorapatite crystals grown from this flux method are known to have 3–6% deficiency in $CaCl_2$, but remain monoclinic in symmetry (Prener 1967, Elliott *et al.* 1975).

Approximately ~100 mg powder and three selected crystals of synthetic chlorapatite were annealed at 1300°C and atmospheric pressure for two hours.

The EPR experiments

All X-band EPR experiments were performed on a Bruker ESP300E spectrometer at the Department of Chemistry, University of Saskatchewan. Powder samples were prepared by grinding hand-picked grains of chlorapatite and then were subjected to 4 hours gamma irradiation at room temperature on a ^{60}Co cell at a rate of 2260 Rad/min. Powder X-band EPR spectra at room temperature were collected by use of a Bruker T110 rectangular cavity with a field-modulation frequency of 100 kHz and a microwave power of 15 dB. Powder X-band EPR spectra at elevated temperatures (from 31 to 323°C with intervals of 30 to 40°C) were obtained by use of a Bruker high-T cavity at the same modulation frequency and microwave power. Calibration of the magnetic field was made by use of 2,2-Diphenyl-picrylhydrazyl (DPPH).

Single crystals of chlorapatite, selected on the basis of clarity, size and morphology, were irradiated for up to 24 hours on the ^{60}Co source at room temperature. Crystal alignment of chlorapatite was made possible by its well-developed prismatic form {100}. Single-crystal X-band EPR spectra at room temperature were obtained on a Bruker cylindrical cavity for two orthogonal rotation planes (// and ⊥ the crystallographic *c* axis).

Powder and single-crystal W-band EPR spectra of gamma-irradiated chlorapatite were obtained at room temperature on a MARK II spectrometer at the Illinois EPR Research Center, University of Illinois at Urbana-Champaign (Nilges *et al.* 1999). A calibration of the magnetic field for W-band measurements was made by use of Metrolab NMR Teslameter PT2025 (Nilges *et al.* 1999). Simulations of the EPR spectra were performed by use of the software package EPR–NMR (Mombourquette *et al.* 1996).

RESULTS

Powder EPR spectra

The selected grains of synthetic chlorapatite for powder EPR are colorless, transparent and free of melt inclusions. The powder sample of synthetic chlorapatite before irradiation is EPR-silent at the X-band frequency. After 4 hours of gamma irradiation, the powder sample changes to a bluish color. Figure 2 shows that the room-temperature X-band EPR spectrum of the gamma-irradiated chlorapatite reveals at least two hole-like centers, similar to those reported by Knottnerus *et al.* (1972) and Roufosse *et al.* (1974). The EPR spectra of these centers were described (Roufosse *et al.* 1974) by means of the axially symmetrical spin-hamiltonian:

$$\hat{H} = \beta_e[g_{\parallel}S_zB_z + g_{\perp}(S_xB_x + S_yB_y)] \\ + \Sigma_i [A_{\parallel}^{(i)}S_zI_z^{(i)} + A_{\perp}^{(i)}(S_xI_x^{(i)} + S_yI_y^{(i)})] \quad (1)$$

where $g_{\parallel}$ and $g_{\perp}$ are the axially symmetrical g values, $A_{\parallel}$ and $A_{\perp}$ are the hyperfine interaction parameters parallel and perpendicular to the crystal's *c* axis; this axis was found to be an axis of symmetry for both

defect centers. The index "i" runs over the relevant spin-bearing nuclei.

Roufosse *et al.* (1974) noted that center H(I) is characterized by hyperfine interaction with three non-equivalent chlorine nuclei. However, the principal values of the hyperfine-interaction matrix for one Cl nucleus are much larger than those for the other two. The single-crystal work of Roufosse *et al.* (1974) showed that the EPR spectrum at magnetic field **B** perpendicular to the *c* axis consists of four major lines with approximately equal spacing and equal intensity, characteristic of hyperfine interaction with a single spin-3/2 nucleus. Closer examination indicated a second set of four equally spaced lines having intensity about one-third that of the first set and constant splittings of about 0.8 G. These two sets of lines are attributable to hyperfine interaction with the nearest-neighbor chlorine nucleus, which has two magnetic isotopes ^{35}Cl (75.77% natural abundance) and ^{37}Cl (24.23%). Both ^{35}Cl and ^{37}Cl have nuclear spins of 3/2, but their nuclear magnetic g-factors are 0.5479198 and 0.4560854, respectively (Weil *et al.* 1994). For **B** parallel to the *c* axis, additional splittings are observed and have been attributed to hyperfine interactions with two non-equivalent chlorine nuclei (Roufosse *et al.* 1974).

Spectral simulations using spin-hamiltonian parameters (Table 1) from Roufosse *et al.* (1974) confirmed the presence of centers H(I) and H(II). However, these two centers cannot explain all experimentally observed lines, which point to the presence of an additional paramagnetic defect center (Fig. 2).

Figure 3 illustrates that center H(I) persists to at least 155°C but is not observed at 199°C or higher temperatures. Center H(II) is present up to at least

254°C. The disappearance of center H(I) at elevated temperatures discloses the presence of a new hole-like defect center [hereafter referred to as center H(III)]. This center is characterized by an electron spin ½ and hyperfine interaction with a nuclear spin ^{3}/$_2$, and has uniaxial symmetry. This center is responsible for the extra lines observed in the room-temperature X-band EPR spectrum, but is partly overlapped with center H(I) (Fig. 2).

All three of these hole-like centers show appreciable line broadening with increasing temperature. Figure 4 shows that the linewidths of centers H(I) and H(II) grow exponentially with temperature, whereas that of H(III) is not very sensitive to temperature below 300°C. Above 300°C, center H(III) experiences significant line broadening, leading to a low signal-to-noise ratio (Fig. 3).

Following the *in situ* high-T X-band EPR measurements, the chlorapatite powder was allowed to cool

TABLE 1. SPIN-HAMILTONIAN PARAMETERS FOR DEFECT CENTERS
IN GAMMA-IRRADIATED CHLORAPATITE

	Center H(I)	Center H(II)	Center H(III)	Center E(I)
$g_\parallel$	2.0031(2)	2.0032	2.0037	1.9985
$g_\perp$	2.0256(2)	2.0386	2.0197	2.000
$A_\parallel^{(1)}/g_e\beta_e$	30.3	No	24.3	1.05
$A_\perp^{(1)}/g_e\beta_e$	14.8	observed	10.5	<0.5
$A_\parallel^{(2)}/g_e\beta_e$	1.55	hyperfine		
$A_\perp^{(2)}/g_e\beta_e$	0.8	structure		
$A_\parallel^{(3)}/g_e\beta_e$	0.94			
$A_\perp^{(3)}/g_e\beta_e$	0.4			

Magnitudes for the A components are given for the ^{35}Cl isotope in Gauss. The parameters for centers H(I) and H(II) were taken from Roufosse *et al.* (1974).
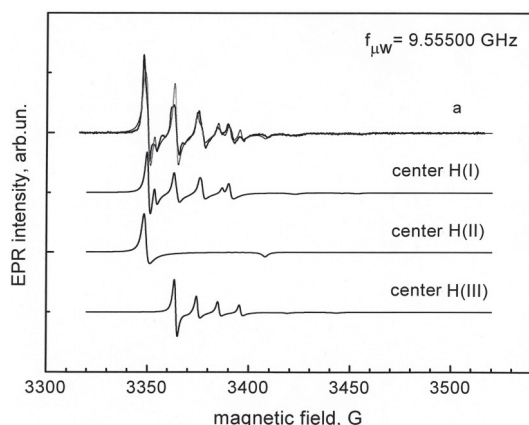

FIG. 2. Comparison of observed room-temperature EPR powder X-band spectrum (solid line) with a simulated spectrum (dotted line) of gamma-irradiated chlorapatite. Also shown are the simulated spectra of centers H(I), H(II), and H(III).
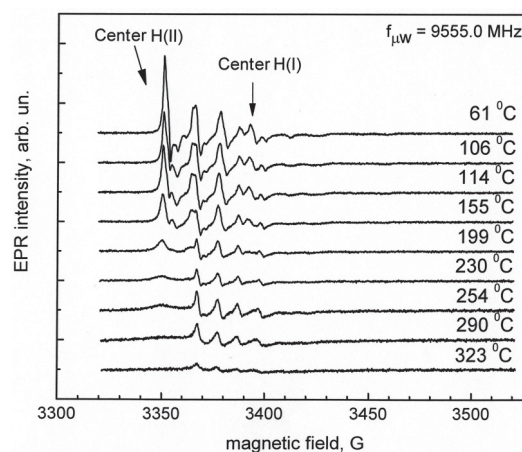

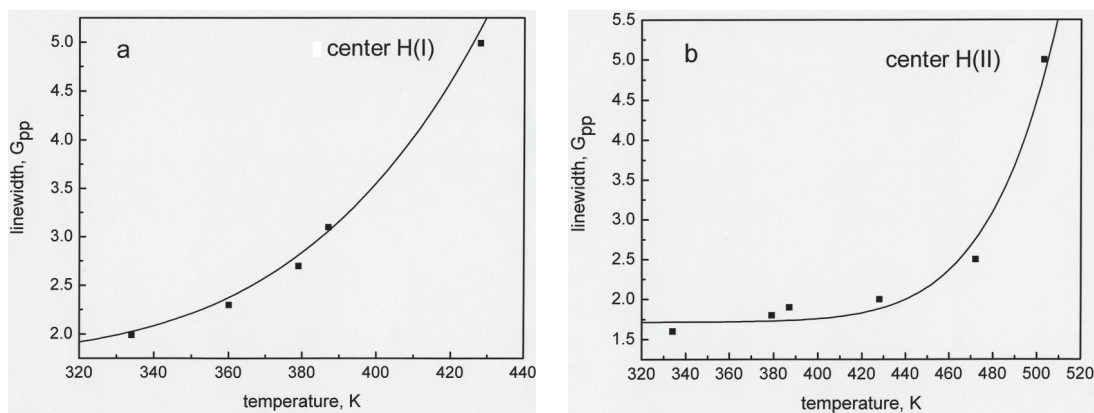FIG. 3. Powder X-band EPR spectra of gamma-irradiated chlorapatite at elevated temperatures.

FIG. 4. Temperature dependence of linewidths for centers: (a) H(I) and (b) H(II). Here, linewidths were determined by spectral simulations.

to room temperature. Re-measurement at room temperature showed that all three hole-like defect centers remain active. However, centers H(I) and H(II) were bleached after annealing at 500°C for two hours, and H(III) was bleached after annealing at 600°C for two hours.

The powder W-band EPR spectrum (Fig. 5) of gamma-irradiated chlorapatite clearly discloses the presence of H(III) in addition to H(I) and H(II). Center H(III) is now well separated in field position from both centers H(I) and H(II).

Single-crystal EPR spectra

The single crystals of flux-grown chlorapatite are dark in color immediately after gamma irradiation, but change to a red color after exposure to daylight. These red crystals are EPR-silent. Therefore, crystals were kept in the dark to prevent this color change after gamma irradiation and during EPR experiments. The single-crystal X-band EPR spectra of gamma-irradiated chlorapatite reveal a new uniaxial spin-1/2 defect center (Fig. 6), which can be described by the spin-hamiltonian (1). The symmetry axis of this center coincides with the c crystallographic axis. The EPR spectrum of this center with the external magnetic field parallel to the c crystallographic axis has a quite complicated form. However, one can distinguish seven equally spaced EPR lines (Fig. 6a). The intensity proportion of these lines is (1 : 2.11 : 3.58 : 4.18 : 3.4 : 2.15 : 1.01), consistent with hyperfine interaction of an unpaired electron with two equivalent ^{35}Cl nuclei. The minor deviation of the observed intensity-proportion from the theoretically expected value (1 : 2 : 3 : 4 : 3 : 2 : 1) for an unpaired electron interacting with two equivalent 3/2 nuclei is
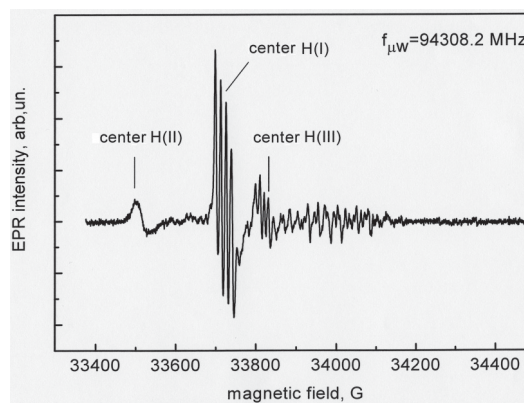

FIG. 5. Powder room-temperature W-band EPR spectrum of gamma-irradiated chlorapatite.

most likely attributable to minor contributions from the less abundant ^{37}Cl isotope. The seven lines are well resolved only where the magnetic field is within 30° of the c crystallographic axis (Fig. 6a) and merge into one broad line where the magnetic field is perpendicular to the c axis (Fig. 6b).

EPR spectra of annealed chlorapatite

EPR spectra of an annealed sample of chlorapatite powder in air at 1300°C for 2 hours were taken at room temperature. This annealed sample exhibited only center H(II) after gamma irradiation, whereas H(I) and H(III) have disappeared.

Discussion

Hole-like centers

Centers H(I) and H(II) observed in this study are the same as those reported by Knottnerus *et al.* (1972) and Roufosse *et al.* (1974). The single-crystal spectra of these two centers in Knottnerus *et al.* (1972) and Roufosse *et al.* (1974) are similar. However, these authors reported different spin-hamiltonian parameters, and proposed different structural models for these two centers (Fig. 7). Our spectral simulations support the spin-hamiltonian parameters reported by Roufosse *et al.* (1974). Moreover, our spectral simulations (Fig. 2) also reveal the presence of center H(III) with spin-hamiltonian parameters given in Table 1. The presence of center H(III) is confirmed by high-T X-band and W-band measurements (Figs. 3, 5).

Roufosse *et al.* (1974) showed that the EPR spectra of center H(I) are characterized by hyperfine interaction with three non-equivalent ^{35}Cl nuclei. The spin-hamiltonian parameters for center H(I) suggest a structural model consisting of a hole shared primarily between an O^{2-} impurity (in substitution for a Cl^- ion) and one of the two adjacent chlorine ions in the anion column. (*i.e.*, Cl^1; Fig. 7). Also, there is a small electronic density of unpaired electron on the other chlorine ion adjacent to the O^{2-} ion (Cl^2) and on the next-nearest-neighbor chlorine ion (Cl^3; Fig. 7). Our powder X-band EPR spectrum only discloses the largest hyperfine splitting, whereas the high-field lines corresponding to $g_\parallel$ are almost twice as broad as the $g_\perp$ lines. This is consistent with the spin-hamiltonian parameters of Roufosse *et al.* (1974), which predict that hyperfine splitting caused by the second ^{35}Cl nucleus is 1.55 G for B parallel to the

c axis but is reduced to only 0.8 G for B perpendicular to the *c* axis.

The most salient feature of center H(II) is that hyperfine interaction with neighboring chlorine nuclei is not observed. Knottnerus *et al.* (1972) first proposed that a hole is trapped by two substitutional oxygen ions (*i.e.*, formation of an O_2^{3-} molecular ion) sandwiched between two chlorine vacancies. In this model, no significant hyperfine splitting is expected because the neighbor chlorine nuclei are missing. The structural model of Roufosse *et al.* (1974) consists of a hole trapped on one substitutional oxygen ion (*i.e.*, the formation of an O^- ion) adjacent to a chlorine vacancy (Fig. 7). Roufosse *et al.* (1974) suggested that the relaxation of the O^- ion towards the center of the vacancy accounts for a negligibly small hyperfine splitting with the neighboring ^{35}Cl nucleus.

The g-factor values of center H(III) are similar to those of centers H(I) and H(II) (Table 1), suggesting that H(III) is also associated with a hole trapped by a substitutional oxygen ion in the anion column. The characteristic hyperfine splitting (Figs. 2, 5) suggests that H(III) consists of a hole next to a Cl^- ion vacancy (Fig. 7). Indeed, if the hole is trapped by an oxygen ion, hyperfine splitting from the nearest-neighbor ^{35}Cl nucleus is expected to be smaller than that for center H(I), in which the trapped hole is shared between a substitutional oxygen ion and an adjacent chlorine ion (Roufosse *et al.* 1974). Therefore, our structural model for H(III) is the same as that proposed for H(II) by Roufosse *et al.* (1974). This result leads us to favor the structural model of Knottnerus *et al.* (1972) for center H(II). This two-vacancy arrangement is more symmetrical than the one-vacancy model of Roufosse *et al.* (1974). The crystal-field splitting from this symmetrical
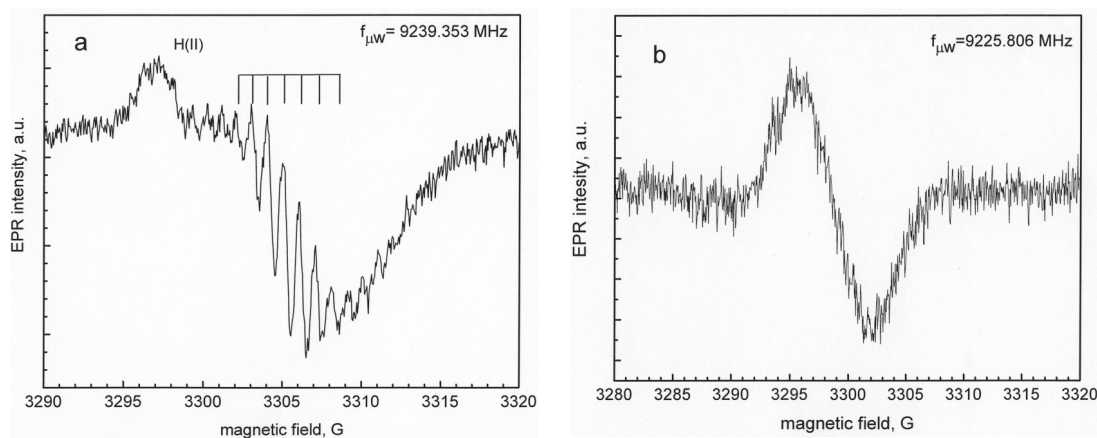

FIG. 6. Single-crystal RT X-band EPR spectra of gamma-irradiated chlorapatite at magnetic field (a) parallel and (b) perpendicular to the *c* crystallographic axis.

arrangement is expected to be smaller than that for center H(III). An alternative structural model for center H(II), consisting of a hole trapped by one substitutional oxygen ion sandwiched between two Cl⁻ vacancies, which can explain the lack of hyperfine interaction, is considered unlikely, because a (VOV) defect has one positive charge and is unlikely to be the precursor for a hole-like center.

The structural models of centers H(I), H(II), and H(III) in chlorapatite can be evaluated further using the results of annealing experiments. Annealing experiments at 1300°C and atmospheric pressure are expected to create additional chlorine vacancies and oxygen ions in the anion column of chlorapatite. Also, vacancies and oxygen ions in the anion column are known to be highly mobile at elevated temperatures (Farver & Giletti 1989) and to form clusters. Therefore, the disappearance of centers H(I) and H(III) and the persistence of center H(II) in annealed chlorapatite provide further support for the proposed structural models of these centers.

The temperature dependence of the EPR linewidth for centers H(I) and H(II) can be fitted with an exponential law: $\Delta B_{pp}(T) = \Delta B_{pp}(T_o) \exp(-\varepsilon/kT)$ (see Fig. 4). The fitted ε values are ~0.33 and ~0.72 eV for centers H(I) and H(II). The fitted ε value for this center H(II) is similar to the crystal-field splitting energy calculated from the g factors (i.e., 0.74 eV). Thus, the Orbach mechanism (Abragam & Bleaney 1970) is dominant in this temperature range [i.e., $1/T_1 \simeq \exp(-\Delta/kT)$, where Δ is the crystal-field splitting energy]. Therefore, the temperature dependence of the linewidth for center H(II) is consistent with the change of the spin-lattice relaxation time. However, the fitted ε value of center H(I) is much less than the calculated crystal-field splitting energy (i.e., 1.28 eV). We suspect that the spin-lattice relaxation time for this center is related to the spin-changing motion of the hole between equivalent Cl⁻ ions adjacent to the substitutional O⁻ ion.

The negligible increase in linewidth for center H(III) below 300°C (not shown) does not allow a precise fit in order to establish temperature dependence. The significant increase in line broadening of this center above ~300°C (Fig. 3) is probably attributable to an approach to the phase transition (cf. Bauer & Klee 1993).

Electron-like center

The single-crystal X-band EPR spectra reveal the presence of a new electron-like defect center (Fig. 6). The electronic nature of this center is suggested by its g-factor values (Table 1), which are less than that for a free electron (2.0023). On the basis of the EPR spectra, we propose that this center contains an electron trapped in an isolated chlorine vacancy in the anion column (Fig. 7). This structural arrangement can explain the observed hyperfine interaction with two neighboring nuclei of chlorine (Fig. 5).

Comparison of radiation-induced defect centers in chlorapatite and fluorapatite

Roufosse et al. (1974) noted that center H(I) in chlorapatite is closely similar to center $^FH(II)$ in fluorapatite (Piper et al. 1965). Roufosse et al. (1974) emphasized that the lower symmetry of chlorapatite (i.e., location of Cl⁻ ions away from the mirror plane) causes asymmetry in the location of the trapped hole in the anion column. They showed that this asymmetry is responsible for the magnetic non-equivalence of neighboring Cl nuclei, whereas the two neighboring F nuclei in center $^FH(II)$ (Segall et al. 1962) in fluorapatite remain equivalent. The structural model for center H(III) in chlorapatite corresponds to that of center $^FH(I)$ in fluorapatite. It is surprising, therefore, that center $^FH(I)$ in fluorapatite is stable only below 225 K (Piper et al. 1965), whereas center H(III) in chlorapatite is stable up to at least 323°C (Fig. 2). There is not an equivalent hole-like center in fluorapatite to center H(II) in chlorapatite.

The new electronic center E(I) in chlorapatite is equivalent to center $^FE(II)$ in fluorapatite (Piper et al. 1965). Several authors (Johnson 1961, Swank 1964, Piper et al. 1965) noted that center $^FE(II)$ in fluorapatite is closely comparable to the well-known F center in alkali halides. Piper et al. (1965) correlated an optical absorption band at ~450 nm in fluorapatite to center $^FE(II)$. Similarly, Knottnerus et al. (1972) observed an optical absorption band of ~450 nm in chlorapatite at 5 K and, by analogy with fluorapatite, attributed this absorption band to an F-like center. The present study first confirms such an F-like center in chlorapatite. Moreover, the presence of both an F-like center and center H(III) may account for the red color of gamma-irradiated chlorapatite crystals after exposure to daylight, because these centers may recombine to form a diamagnetic center (e.g., one equivalent to center ^FB in fluorapatite; Piper et al. 1965).
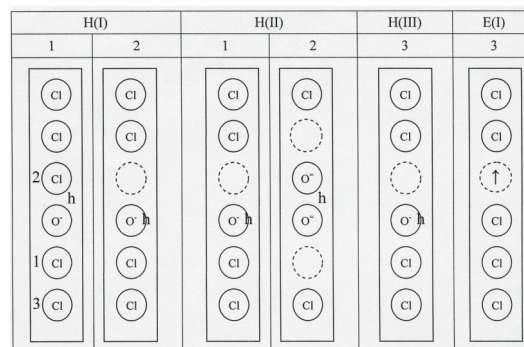

FIG. 7. Structural models of the radiation-induced centers in chlorapatite: (1) proposed by Roufosse et al. (1974), (2) proposed by Knottnerus et al. (1972), (3) this study. Symbol "↑" represents a trapped electron; "h", a trapped hole.

Finally, the presence of a minor amount of U in the flux-grown chlorapatite is unlikely to be responsible for the paramagnetic centers reported in this study, because these centers are not detected in samples without irradiation. Also, U is known to be present at similar levels in both single crystals and powder samples. The common presence of hole-like centers in powders is probably attributable to the abundance of substituted oxygen ions in those samples, whereas single crystals may contain more isolated vacancies that give rise to electron-like centers.

REFERENCES

ABRAGAM, A. & BLEANEY, B. (1970): *Electron Paramagnetic Resonance of Transition Ions*. Clarendon Press, Oxford, U.K.

BAUER, M. & KLEE, W.E. (1993): The monoclinic-hexagonal phase transition in chlorapatite. *Eur. J. Mineral.* **5**, 307-316.

ELLIOTT, J.C. (1994): *Structure and Chemistry of the Apatites and Other Calcium Orthophosphates*. Elsevier, Amsterdam, The Netherlands.

_____, YOUNG, K.A & MACKIE, P.E. (1975): Effect of chlorine ion vacancies on the local atomic parameters in nonstoichiometric chlorapatite. *Acta Crystallogr.* **A31**, S268.

FARVER, J.R. & GILETTI, B.J. (1989): Oxygen and strontium diffusion kinetics in apatite and potential application to thermal history determinations. *Geochim. Cosmochim. Acta* **53**, 1621-1631.

HUGHES, J.M. & RAKOVAN, J. (2002): The crystal structure of apatite, $Ca_5(PO_4)_3(F,OH,Cl)$. *In* Phosphates – Geochemical, Geobiological, and Materials Importance (M.L. Kohn, J. Rakovan & J.M. Hughes, eds.). *Rev. Mineral. Geochem.* **48**, 1-12.

JOHNSON, P.D. (1961): Some optical properties of powder and crystal halophosphate phosphors. *J. Electrochem. Soc.* **108**, 159-162.

KNOTTNERUS, D.I.M., DEN HARTOG, H.W. & VAN DER LUGT, W. (1972): Optical and EPR investigations of colour centres in calcium chlorapatite. *Phys. Stat. Sol.*(a) **13**, 505-515.

MCCONNELL, D. (1973): *Apatite, its Crystal Chemistry, Mineralogy, Utilization, and Geologic and Biologic Occurrences*. Springer-Verlag, New York, N.Y.

MENGEOT, M., BARTRAM, R.H. & GILLIAM, O.R. (1975): Paramagnetic hole-like defect in irradiated calcium hydroxyapatite single crystals. *Phys. Rev.* **B11**, 4110-4124.

MOMBOURQUETTE, M.J., WEIL, J.A. & MCGAVIN, D.G. (1996): *EPR–NMR* (*Users' Manual*). Department of Chemistry, University of Saskatchewan, Saskatoon, Saskatchewan, Canada.

NILGES, M.J., SMIRNOV, A.I., CLARKSON, R.B. & BELFORD, R.L. (1999): Electron paramagnetic resonance W-band spectrometer with a low-noise amplifier. *Appl. Magn. Res.* **16**, 167-183.

PAN, YUANMING & FLEET, M.E. (2002): Compositions of the apatite-group minerals: substitution mechanisms and controlling factors. *In* Phosphates – Geochemical, Geobiological, and Materials Importance (M.L. Kohn, J. Rakovan & J.M. Hughes, eds.). *Rev. Mineral. Geochem.* **48**, 13-49.

PIPER, W.W., KRAVITZ, L.C. & SWANK, R.K. (1965): Axially symmetric paramagnetic color centres in fluorapatite. *Phys. Rev.* **138**, A1802-A1814.

PRENER, J.S. (1967): The growth and crystallographic properties of calcium fluor- and chlorapatite. *J. Electrochem. Soc.* **114**, 77-83.

ROUFOSSE, A., STAPELBROEK, M., BARTRAM, R.H. & GILLIAM, O.R. (1974): Oxygen-associated hole-like centers in calcium chlorapatite. *Phys. Rev.* **B9**, 855-862.

SEGALL, B., LUDWIG, G.W., WOODBURY, H.H. & JOHNSON, P.D. (1962): Electron spin resonance of a centre in calcium fluorophosphate. *Phys. Rev.* **128**, 76-79.

SWANK, R.K. (1964): Color centres in X-irradiated halophosphate crystals. *Phys. Rev.* **135**, A266-A275.

WARREN, R.W. (1972): Defect centres in calcium fluorophosphate. *Phys. Rev. B* **6**, 4679-4689.

WEIL, J.A., BOLTON, J.R. & WERTZ, J.F. (1994): *Electron Paramagnetic Resonance: Elementary Theory and Practical Applications*. John Wiley & Sons, New York, N.Y.